

Development of a Dataset of the Spatiotemporal Distribution of Typical Salt Marsh Vegetation in the Yellow River Delta (1999–2020)

Hu, J. F.^{1,2,3} Gong, Z. N.^{*1,2,3,4} Zhang, C.^{1,2} Qiu, H. C.^{1,2,3}

1. College of Resources, Environment and Tourism, Capital Normal University, Beijing 100048, China;
2. Key Laboratory of 3D Information Acquisition and Application of Ministry, Beijing 100048, China;
3. Beijing Key Laboratory of Resources Environment and GIS, Beijing 100048, China;
4. Beijing Laboratory of Water Resources Security, Beijing 10048, China

Abstract: The typical salt marsh vegetation in the Yellow River Delta, which is represented by *Suaeda salsa*, *Phragmites australis*, and *Spartina alterniflora*, provides a variety of ecological services such as maintaining biodiversity, providing important habitats, reducing storm runoff, and regulating the climate. The study of its distribution and succession is of great significance for the conservation and management of the entire ecosystem. A dataset of the typical salt marsh vegetation in the Yellow River Delta was created and analyzed. Based on 2068 Landsat TM/ETM/OLI, Sentinel-2 MSI optical data, and Sentinel-1 SAR data from 1999 to 2020, a comprehensive set of salt marsh vegetation features during the entire growth period was constructed used the Google Earth Engine platform. The best feature combination was selected using the recursive feature elimination feature optimization algorithm and was applied in a random forest classification model to obtain the final map. Then, the spatial-temporal distribution dataset of typical salt marsh vegetation was analyzed. The dataset mainly covers the estuarine wetlands of the Yellow River Delta, with spatial resolutions of 10 m and 30 m. The data storage is in .tif format, and the projection coordinate system is WGS_1984_UTM_Zone_50N. It contains 16 data files, and the amount of data is 143 MB (2.41 MB is compressed into one file).

Keywords: Yellow River Delta; salt marsh vegetation; long time series; feature optimization algorithm

DOI: <https://doi.org/10.3974/geodp.2022.02.07>

CSTR: <https://cstr.science.org.cn/CSTR:20146.14.2022.02.07>

Dataset Availability Statement:

The dataset supporting this paper was published and is accessible through the *Digital Journal of Global Change Data Repository* at: <https://doi.org/10.3974/geodb.2022.01.06.V1> or <https://cstr.science.org.cn/CSTR:20146.11.2022.01.06.V1>.

Received: 10-02-2022; **Accepted:** 16-05-2022; **Published:** 25-06-2022

Foundation: Ministry of Science and Technology of P. R. China (2017YFC0505900)

***Corresponding Author:** Gong, Z. N., Capital Normal University, gongzhn@163.com

Data Citation: [1] Hu, J. F., Gong, Z. N., Zhang, C., *et al.* Development of a dataset of the spatiotemporal distribution of typical salt marsh vegetation in the Yellow River Delta (1999–2020) [J]. *Journal of Global Change Data & Discovery*, 2022, 6(2): 217–224. <https://doi.org/10.3974/geodp.2022.02.07>. <https://cstr.science.org.cn/CSTR:20146.14.2022.02.07>.

[2] Hu, J. F., Gong, Z. N., Zhang, C., *et al.* Spatial-temporal dataset of salt marsh vegetation in Yellow River Delta (1999–2020) [J/DB/OL]. *Digital Journal of Global Change Data Repository*, 2022. <https://doi.org/10.3974/geodb.2022.01.06.V1>. <https://cstr.science.org.cn/CSTR:20146.11.2022.01.06.V1>.

1 Introduction

Estuarine wetlands are the frontier area of sea-land interactions and are one of the most important components of coastal ecosystems^[1]. The structure and layout of wetland vegetation can reflect the basic characteristics of and changes in the wetland ecological environment, which is of great significance to monitoring and studying regional ecological environment changes. The salt marsh vegetation in an estuarine wetland has ecological functions such as energy exchange, biological habitats, and environmental improvement^[2]. Accurate extraction of its distribution information and timely analysis of its dynamic changes are of great significance to the protection and management of the wetland ecological environment and even to the regional ecological environment^[3].

The Yellow River Delta wetland, which is located in the coastal area and water crisscross zone, is a typical coastal wetland ecosystem with a high sensitivity and vulnerability. Under the context of global warming, species invasion, and human activities, the surface morphology of the Yellow River Delta has undergone significant evolution. In addition, native species such as *P. australis* and *S. salsa* face the problems of habitat fragmentation and area reduction, while the invasive species *S. alterniflora* has rapidly colonized and expanded due to its own competitive advantage. As a result, the distribution pattern of estuarine wetland vegetation has exhibited frequent succession^[3]. Accurate and effective extraction of estuarine wetland salt marsh vegetation information has always been an urgent problem to be solved. The solution to this problem is of great significance to the monitoring and protection of the ecological environment of the Yellow River Delta wetland^[4]. In this study, the estuary of the Yellow River Delta is taken as the study area. Based on the characteristics of the phenological season of the salt marsh vegetation, 2068 Landsat TM/ETM/OLI scenes, Sentinel-2 MSI optical data, and Sentinel-1 SAR data were fully used in the Google Earth Engine (GEE) big data platform. The spatial distribution data of the typical salt marsh plant populations in the Yellow River Delta were obtained, and then, spatial and temporal distribution datasets of typical salt marsh plant populations from 1999 to 2020 were obtained by mining and analyzing their distribution characteristics.

2 Metadata of the Dataset

Table 1 lists the name, author, geographical region, data age, temporal resolution, spatial resolution, composition of the dataset, data publishing and sharing service platform, and data sharing policy of the Spatial-temporal dataset of salt marsh vegetation in Yellow River Delta (1999–2020)^[5].

3 Development Methods of the Dataset

In this study, all of the available Landsat series data of a good quality (cloud cover <30%), Sentinel-2 optical data, and Sentinel-1 SAR data from 1999 to 2020, including 197 Landsat-7 enhanced thematic mapper plus (ETM+) images, 62 Landsat-8 OLI images, 1,294 Sentinel-2 MSI images, and 515 Sentinel-1 SAR images, were selected. The GEE cloud platform (<https://earthengine.google.com/>) integrates a large amount of remote sensing image data and other data resources. Landsat series satellite remote sensing data from 1972 to present, MODIS data and its series products from 2000 to present, Sentinel series satellite remote sensing data from 2014 to present, and global scale elevation, meteorology, and land use data can be called online^[7]. All of the image data used in this study can be invoked on the GEE platform. The other auxiliary analysis data included measured sample data for the Yellow River Delta Nature Reserve, which were collected by our research group several times

Table 1 Metadata summary of Spatial-temporal dataset of salt marsh vegetation in Yellow River Delta (1999–2020)

Items	description
Dataset full name	Spatial-temporal distribution dataset of typical salt marsh vegetation in the Yellow River Delta (1999–2020)
Dataset short name	SaltMarshVegYRD1999-2020
Authors	Hu, J. F., Capital Normal University, 2190902115@cnu.edu.cn Gong, Z. N., Capital Normal University, gongzhn@163.com Zhang, C., Capital Normal University, chzhang_hn@163.com Qiu, H. C., Capital Normal University, qiu_huachang@163.com
Geographical region	Estuarine wetlands at the mouth of the Yellow River Delta
Year	1999–2020
Temporal resolution	year
Spatial resolution	30 m, 10 m
Data format	.shp, .tif, .xlsx
Data size	172 MB (Compressed to a single file, 31.7 MB)
Data files	64
Foundation	Ministry of Science and Technology of P. R. China (2017YFC0505900)
Data computing environment	ENVI, ArcGIS
Data publisher	Global Change Research Data Publishing & Repository, http://www.geodoi.ac.cn
Address	No. 11A, Datun Road, Chaoyang District, Beijing 100101, China
Data sharing policy	Data from the Global Change Research Data Publishing & Repository includes metadata, datasets (in the <i>Digital Journal of Global Change Data Repository</i>), and publications (in the <i>Journal of Global Change Data & Discovery</i>). Data sharing policy includes: (1) Data are openly available and can be free downloaded via the Internet; (2) End users are encouraged to use Data subject to citation; (3) Users, who are by definition also value-added service providers, are welcome to redistribute Data subject to written permission from the GCdataPR Editorial Office and the issuance of a Data redistribution license; and (4) If Data are used to compile new datasets, the ‘ten per cent principal’ should be followed such that Data records utilized should not surpass 10% of the new dataset contents, while sources should be clearly noted in suitable places in the new dataset ^[6]
Communication and searchable system	DOI, CSTR, Crossref, DCI, CSCD, CNKI, SciEngine, WDS/ISC, GEOSS

in recent years. The spectral data for the salt marsh vegetation in different growth states were collected using an ASD FieldSpec 3 back-mounted spectrometer with a spectral range of 350–2,500 nm. In addition, to avoid deviation of the sample point selection caused by environmental changes, the high-precision sample point data were supplemented with visual interpretation results for high-resolution remote sensing Google Earth images.

Using the GEE cloud platform, the radiometric calibration and atmospheric correction of the Landsat 7/8 data and Sentinel-2 data, the terrain correction of the Sentinel-1 data, and the other preprocessing step were realized through coding. Based on the multi-temporal characteristics and life history differences of wetland plants, multiple time-series vegetation indices were calculated on an annual average scale to form a temporal-spectral dimension feature set. The temporal-spatial dimensional feature set was constructed by extracting the backscatter coefficients from the Sentinel-1 data. According to the dynamic changes in the vegetation distribution in the Yellow River Delta in recent years and the quality and availability of the satellite data, we used the Sentinel-1 data to perform co-classification of the temporal-spatial-spectral multi-dimensional features from 2014 to 2020, and the temporal-spectral dimensional features for 1999–2013 were extracted based on historical Landsat time-series data.

Multi-dimensional feature extraction makes full use of the temporal, optical, and spatial texture features of the vegetation, which can effectively improve the accuracy of the classi-

fication; however, the data redundancy caused by the higher dimensional feature sets still creates some problems. In this study, recursive feature elimination (RFE) was adopted to reduce the dimensionality of the feature sets, eliminate the redundant bands, and obtain the best feature combination. The implementation process of the RFE algorithm used in this study is summarized below.

Step 1: Train a random forest algorithm.

Step 2: Calculate the importance measure of the permutation.

Step 3: Eliminate the irrelevant variables.

Step 4: Repeat steps 1 through 3 until the final set of features is obtained. The prediction of the importance of a given variable's permutation depends strongly on its correlations with the other variables.

4 Data Results and Validation

4.1 Dataset Composition

This dataset consists of the following data: (1) the spatial distribution of the salt marsh vegetation in the Yellow River Delta from 1999 to 2020; (2) the distribution frequency of *S. alterniflora* in the Yellow River Delta from 1999 to 2020; (3) the frequency data for *S. salsa* in the Yellow River Delta from 1999 to 2020; and (4) the distribution frequency data for *P. australis* in the Yellow River Delta from 1999 to 2020.

Among them, in the spatial distribution data for the salt marsh vegetation in the Yellow River Delta, the "value" field represents the different salt marsh vegetation classifications. A value of 1 indicates *S. alterniflora*, a value of 2 indicates *S. salsa*, and a value of 3 indicates *P. australis*.

4.2 Data Results

Based on the multi-dimensional feature extraction method and random forest classification algorithm established above, as well as the GEE big data processing platform, Landsat TM/ETM+/OLI data, Sentinel-2 MSI optical images, and Sentinel-1 SAR data for 2068 scenes were used. A spatial-temporal distribution dataset of the typical salt marsh vegetation in the Yellow River Delta from 1999 to 2020 was obtained. The spatial resolution of the dataset was 30 m and 10 m, and its size was 171 MB.

The Yellow River Delta wetland is subject to the combined effects of both marine and Yellow River runoff sediments, resulting in frequent alternating changes in the erosion and deposition. Its ecosystem is sensitive and fragile, with frequent vegetation succession^[10]. Figure 1 shows the long time-series distribution of the typical salt marsh vegetation in the Yellow River Delta. The vegetation distribution has exhibited significant gradient distribution characteristics, while the Yellow River Delta wetland remains in a highly dynamic state. The main salt marsh vegetation in the study area, *P. australis* and *S. salsa*, exhibited a banded pattern from the inland area to the sea before the invasion of *S. alterniflora*. The development of *P. australis* mainly extended along the river, the vegetation evolved toward a more suitable salt environment, i.e., along the river and toward the sea, and *S. salsa* became the pioneer species in the intertidal sea transition zone. Under the disturbance of the estuarine wetland ecosystem by the invasive species, the development and evolution of the typical salt marsh vegetation in the Yellow River Delta have developed new characteristics.

Since 2008, scattered *S. alterniflora* patches have been observed at the coastal edge of the northern bank in the study area. They successfully colonized seagrass beds, exhibiting strong environmental adaptability, and rapidly expanded to occupy the intertidal niche, exhibiting strong interspecies competitiveness. The area colonized reached 1,513.16 ha by 2013

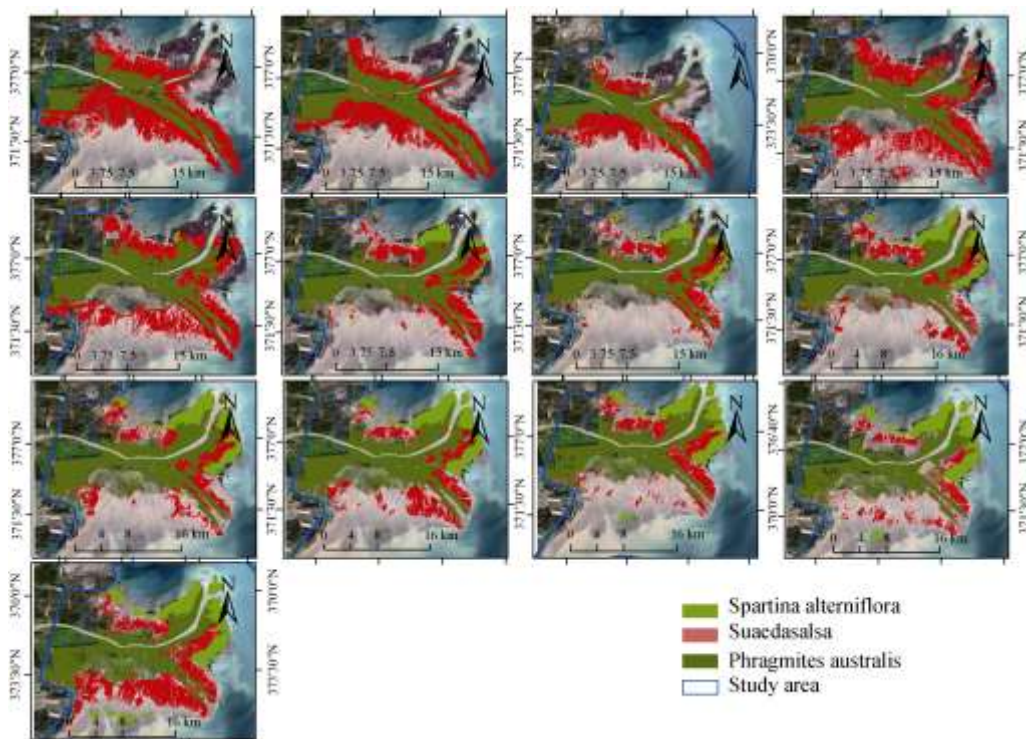


Figure 1 Spatial and temporal distributions of the typical salt marsh vegetation in the Yellow River Delta (1999–2020)

(Figure 2). *S. alterniflora* occupied the most favorable habitats in the coastal wetlands of the Yellow River Delta due to its strong diffusion ability. In addition, the frequent human activities in recent years have led to changes in the distribution structure of the native vegetation communities such as *S. salsa* and *P. australis*, and the native wetlands have been degraded to different degrees. *P. australis* was mainly distributed along the current river channel of the Yellow River and on both sides of the old channel of the Yellow River, extending to the northeast along the current river channel and subsiding to some extent inland along the old channel of the Yellow River. Although it was inferior to *S. alterniflora* in the newly silted plain of the Yellow River estuary, its main distribution was relatively stable. *S. salsa* was a pioneer plant in the muddy tidal flat and high salinity area. However, the deposition and erosion of the estuarine wetland in the Yellow River Delta has been rapid, and *S. salsa* grows poorly under the tidal cycle. Thus, its stability was insufficient, and the area it occupied decreased significantly.

S. alterniflora, with its strong environmental adaptability, formed a large area of single colonies in the southeast where the Yellow River enters the sea, with a total distribution area of 2459.09 ha. The colonization of *S. alterniflora* began in the southernmost plain, and it rapidly

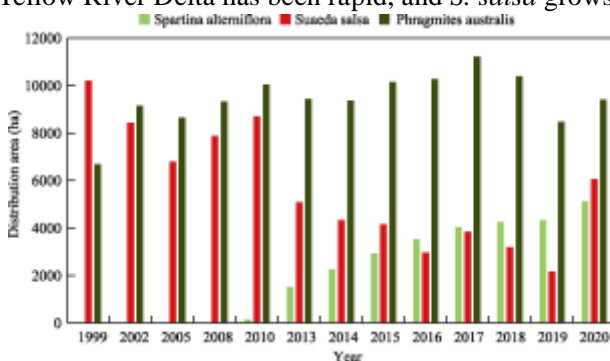


Figure 2 Statistics of typical salt marsh vegetation area

expanded along the east-west direction. By 2020, four spreading patches of *S. alterniflora* were distributed in an east-west band on the southern coastal plain.

Figure 3 shows the distribution frequency of the three typical salt marsh vegetation species. Among them, the red areas had a high annual vegetation occurrence frequency, representing the most suitable ecological niche for growth, while the light green areas had a low growth frequency, and most of these areas were degraded or newly expanded areas with unstable growth. The distribution range of *S. alterniflora* was the smallest among the three plants, but the inter-annual occurrence frequency of *S. alterniflora* was higher within the distribution range, and the distribution range was mostly composed of stable growth area and new expansion area. This is mainly due to the strong reproductive capacity of *S. alterniflora* and its adaptability to wet and saline environments. *S. alterniflora* can generate seeds in order to enter new habitats through sexual reproduction and can form patches to realize the spatial expansion of its population. Once colonization is successful, *S. alterniflora* can rapidly grow suckering plants through asexual reproduction, and thus, the patches of *S. alterniflora* can continuously expand and integrate and can occupy the suitable ecological niche in a continuous peak-plane diffusion. *S. salsa* was widely distributed in the coastal tidal flats, but its distribution frequency was generally low, and most of the areas fluctuated greatly or experienced obvious degradation between years. The stable distribution area was mainly located in the central part of the tidal flat. Although *S. salsa* was a pioneer plant in the muddy tidal flat and heavily saline-alkali areas, its low plant structure and weak rhizomes made it susceptible to environmental stress and lacking in competitive ability, resulting in double inhibition from individual indicators to community indicators. *P. australis* has a wide ecological range of growth and grows in the interaction areas between freshwater, salt water, and salt-fresh water regions. It was distributed in a long and narrow strip along the river bank, extending to the estuary. Its distribution area was also mostly within the stable growth area. According to the distribution frequency of the salt marsh vegetation, in recent years, the regions with a distribution frequency of $\geq 70\%$ were divided into ecological niches suitable for the distribution of typical salt marsh vegetation in the study area. The interannual fluctuations in the salt marsh vegetation in this region were small and the occurrence frequency of the same vegetation type reached 70% during the study period (Figure 4). The area of stable growth of *P. australis* (7,720.41 ha) was the largest, followed by *S. alterniflora* (1,859.66 ha), and that of *Suaeda salsa* (859.26 ha) was the smallest.

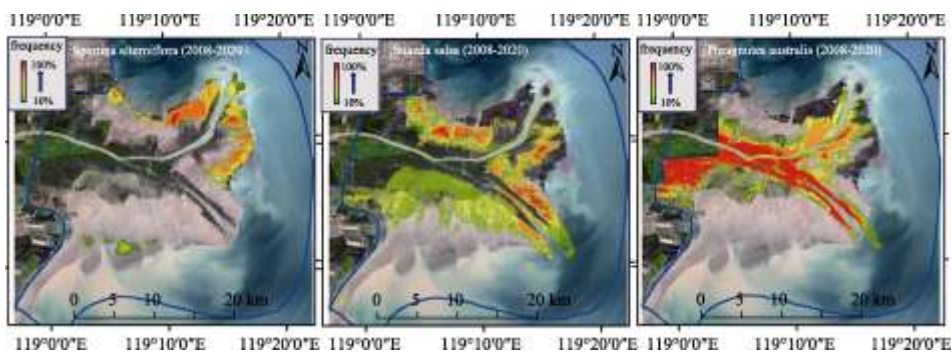


Figure 3 Distribution frequency of typical salt marsh vegetation in the Yellow River Delta (1999–2020)

4.3 Validation of data results

A confusion matrix was used to verify the accuracy of the classification data for the typical salt marsh vegetation in the Yellow River Delta. In the confusion matrix, the value of the

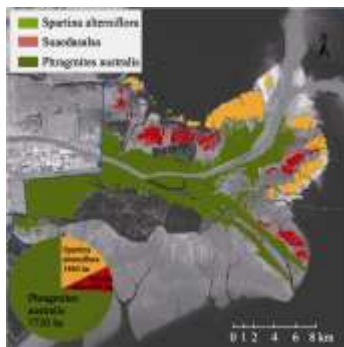


Figure 4 Stable niche distribution of typical salt marsh vegetation in the Yellow River Delta from 1999 to 2020

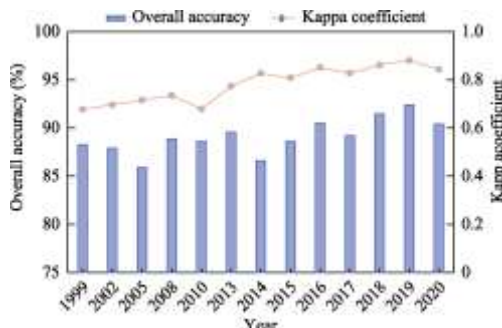


Figure 5 Classification accuracy of typical salt marsh vegetation in the Yellow River Delta from 1999 to 2020

verification sample is compared with the value of the corresponding data result, and an error matrix based on the measured data and the result data is constructed. By calculating the quantitative relationship between the number of correctly classified pixels and the number of total pixels, various extraction accuracy indexes can be obtained. The widely used overall accuracy (OA) and kappa coefficient were used to evaluate and analyze the extraction accuracy of the typical salt marsh vegetation dataset constructed in this study. The overall accuracy is defined as the ratio of the total number of correctly classified pixels to the total number of pixels, and it represents the classification accuracy of the overall pixels. The kappa coefficient can be used to evaluate the quality of the classification, and it can overcome the dependence on the samples and methods caused by using only the accuracy analysis index described above. In addition, it can be used to measure the accuracy of classification. The kappa coefficient was calculated as follows:

$$Kappa = \frac{p_o - p_e}{1 - p_e} \tag{1}$$

$$p_e = \frac{a_1 \times b_1 + a_2 \times b_2 + \dots + a_C \times b_C}{n \times n} \tag{2}$$

where p_o is the total classification accuracy, which is defined as the sum of the correctly classified samples in each category divided by the total number of samples; a_1, a_2, \dots, a_C denotes the real number of samples in each category; b_1, b_2, \dots, b_C denotes the predicted number of samples in each category; and n is the total number of samples. In this study, the time-series images for each year were classified using the GEE platform. During the classification, 70% of the samples were randomly selected to establish a random forest model, and the remaining 30% of the samples were used to verify the results. Figure 5 shows the overall accuracy and kappa coefficient of the typical salt marsh vegetation classification from 1999 to 2020. The overall accuracy ranges from 86% to 92.4%, and the kappa coefficient ranges from 0.68 to 0.88. It can be seen that the classification method used in this study achieved a satisfactory accuracy, and the effect is relatively robust when it is applied to a long time series of data.

5 Discussion and Conclusion

In this study, using the GEE platform, the morphological characteristics and evolution differences of the different types of salt marsh vegetation were fully considered. A total of 2068 Landsat TM/ETM/OLI, Sentinel-2 MSI optical data, and Sentinel-1 SAR data were used to construct the multi-feature space for the entire growth period, and the feature optimization

algorithm of the recursive feature elimination was used to eliminate the redundant features. The classification of the data of typical salt marsh plant populations in the Yellow River Delta from 1999 to 2020 was obtained using a random forest classification algorithm, and the spatial and temporal distribution dataset for the typical salt marsh vegetation was analyzed. Although the Yellow River Delta is the youngest wetland ecosystem in the warm temperate zone in China and the vegetation community is not fully developed and succinct, the coastal wetland in the Yellow River Delta exhibits an obvious hierarchical structure along the river to the sea. The rapid invasion of *S. alterniflora* occupied the ecological niche of *S. salsa*, resulting in local geomorphic changes, which directly and indirectly affected the original ecosystem. The temporal and spatial distribution characteristics of the typical salt marsh vegetation in the Yellow River Delta from 1999 to 2020 were analyzed to provide theoretical and methodological support for the extraction of vegetation information in a wide range of vulnerable estuaries and to provide a scientific basis for ecological restoration and management of the Yellow River Delta protection area.

Author Contributions

Gong, Z. N. made a general design for the development of the dataset; Zhang, C. and Hu, J. F. collected and processed the data, practical models and algorithms, and verified the data. Hu, J. F. wrote data papers and so on.

Conflicts of Interest

The authors declare no conflicts of interest.

References

- [1] He, Y. L., The mechanism of vegetation differentiation in the lower salt marsh of Yangtze River estuary [D]. Shanghai: East China Normal University, 2014.
- [2] Wang, X. H., Li, Y. Z., Meng, H., *et al.* Distribution pattern of plant community in new-born coastal wetland in the Yellow River Delta [J]. *Scientia Geographica Sinica*, 2015, 35(8): 1021–1026.
- [3] Zhang, C., Gong, Z. N., Qiu, H. C., *et al.* Mapping typical Salt-marsh species in the Yellow River Delta wetland supported by temporal-spatial-spectral multidimensional features [J]. *Science of the total environment*, 2021, 783: 147061. DOI: 10.1016/j.scitotenv.2021.147061.
- [4] Zhang, G. H., Wang, R.Y., Zhao, G. X., *et al.* Extraction of vegetation information in coastal ecological vulnerable areas from remote sensing data based on phenology parameters and object-oriented method [J]. *Transactions of the Chinese Society of Agricultural Engineering*, 2018, 34(4):209–216.
- [5] Hu, J. F., Gong, Z. N., Zhang, C., *et al.* Spatial-temporal dataset of salt marsh vegetation in Yellow River Delta (1999–2020) [J/DB/OL]. *Digital Journal of Global Change Data Repository*, 2022. <https://doi.org/10.3974/geodb.2022.01.06.V1>. <https://cstr.escience.org.cn/CSTR:20146.11.2022.01.06.V1>.
- [6] GCdataPR Editorial Office. GCdataPR Data Sharing Policy [OL]. <https://doi.org/10.3974/dp.policy.2014.05> (Updated 2017).
- [7] Wu, Y., Zhou, Z. F., Zhao, X., *et al.* Spatiotemporal variation of vegetation coverage in plateau mountainous areas based on remote sensing cloud computing platform: a case study of Guizhou province [J]. *Carsologica Sinica*, 2020, 39(2): 196–205.
- [8] Breiman, L. Random forests [J]. *Machine Learning*, 2001, 45(1): 5–32.
- [9] Ke, Y. C., Shi, Z. K., Li, P. J., *et al.* Lithological classification and analysis using Hyperion hyperspectral data and Random Forest method [J]. *Acta Petrologica Sinica*, 2018, 34(7): 2181–2188.
- [10] Zhang, X. L. The environmental change and degradation of modern Yellow River Delta coastal wetland [D]. Qingdao: Ocean University of China, 2015.
- [11] Zong, M., Han, G.Q., Li, Y.Z., *et al.* Predicting the potential distribution species of the coastal wetland in the Yellow River Delta, China using MaxEnt model[J]. *Chinese Journal of Applied Ecology*, 2017, 28(06): 1833–1842. DOI:10.13287/j.1001-9332.201706.017.
- [12] Chen, K.X., Cong, P.F., Qu, L.M., *et al.* Simulation of dynamic changes and diffusion of typical vegetation populations in coastal wetlands in the Yellow River Delta. [J]. *Journal of Beijing Normal University(Natural Science)* 2021,57(01):128-134.
- [13] Wang, S.X., Han, L.S., Yang, J., An Improved method of combining multi-indicator desertification classification[J]. *Bulletin of surveying and mapping*, 2021(04):8-12. DOI:10.13474/j.cnki.11-2246.2021.0102.